Electronic Supplementary information

# D-A-D-type bipolar host materials with room temperature phosphorescence for high-efficiency green phosphorescent organic light-emitting diodes

Fei Wang,[a] Jing Sun,[c] Mingli Liu,[b] Huifang Shi,[b] Huili Ma,[b] Wenpeng Ye[b], Hongmei Zhang,[a*] Zhongfu An,[b*] and Wei Huang[a,b]

[a]Key Laboratory for Organic Electronics and Information Displays & Institute of Advanced Materials (IAM), Nanjing University of Posts & Telecommunications, 9 Wenyuan Road, Nanjing 210023, China

[b]Key Laboratory of Flexible Electronics (KLOFE) & Institute of Advanced Materials (IAM), Nanjing Tech University (NanjingTech), 30 South Puzhu Road, Nanjing 211800, China

[c]Key Laboratory of Interface Science and Engineering in Advanced Materials, Taiyuan University of Technology, 79 West Yingze street, Taiyuan 030024, China

*Corresponding author E-mail: iamzfan@njteth.edu.cn, iamhmzhang@njupt.edu.cn

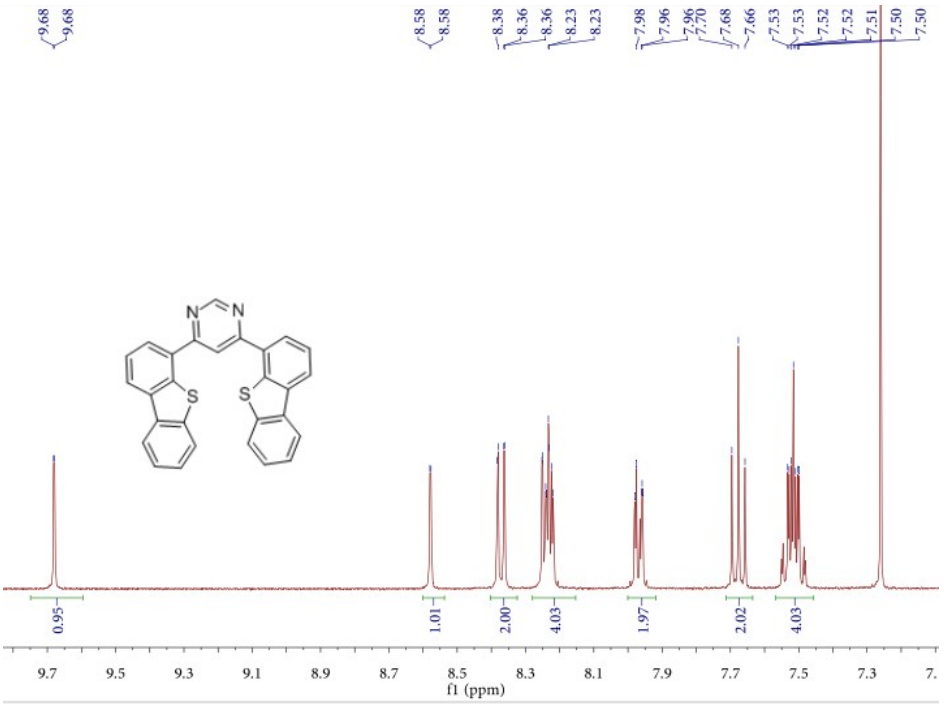


Figure S1. $^{1}H$ NMR spectrum of MDBT in $CDCl_3$.

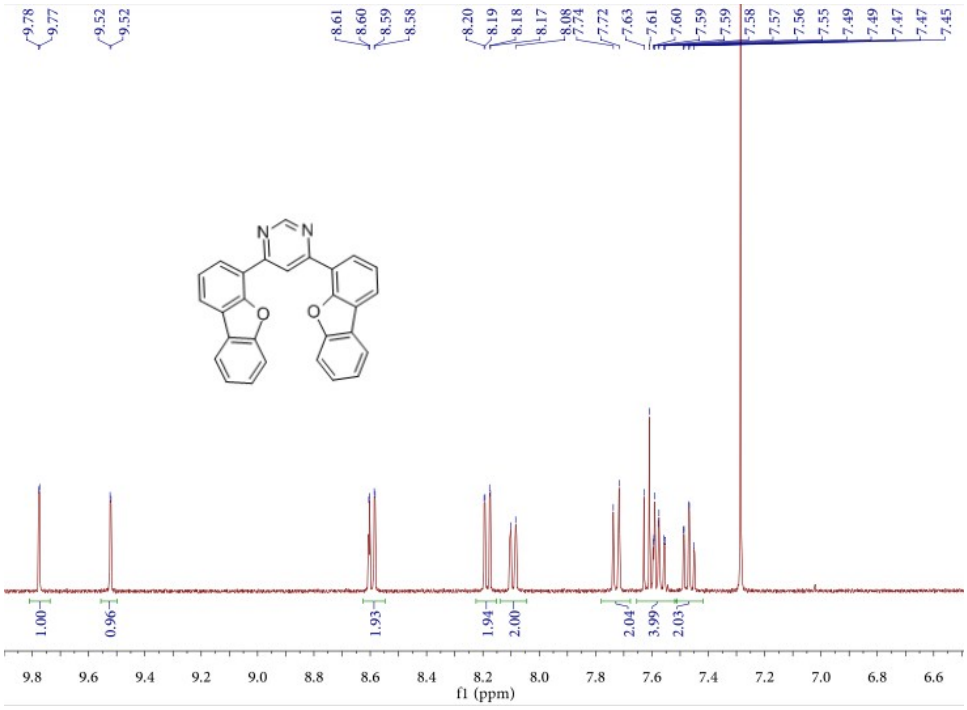


Figure S2. $^{1}H$ NMR spectrum of MDBF in $CDCl_3$.

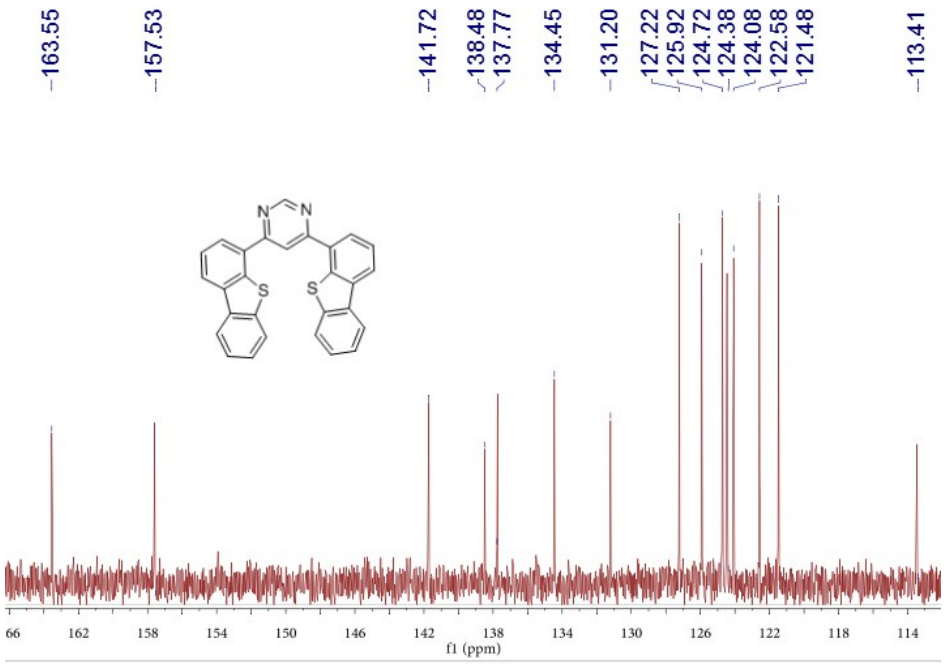


Figure S3. $^{13}C$ NMR spectrum of MDBT in $CDCl_3$.

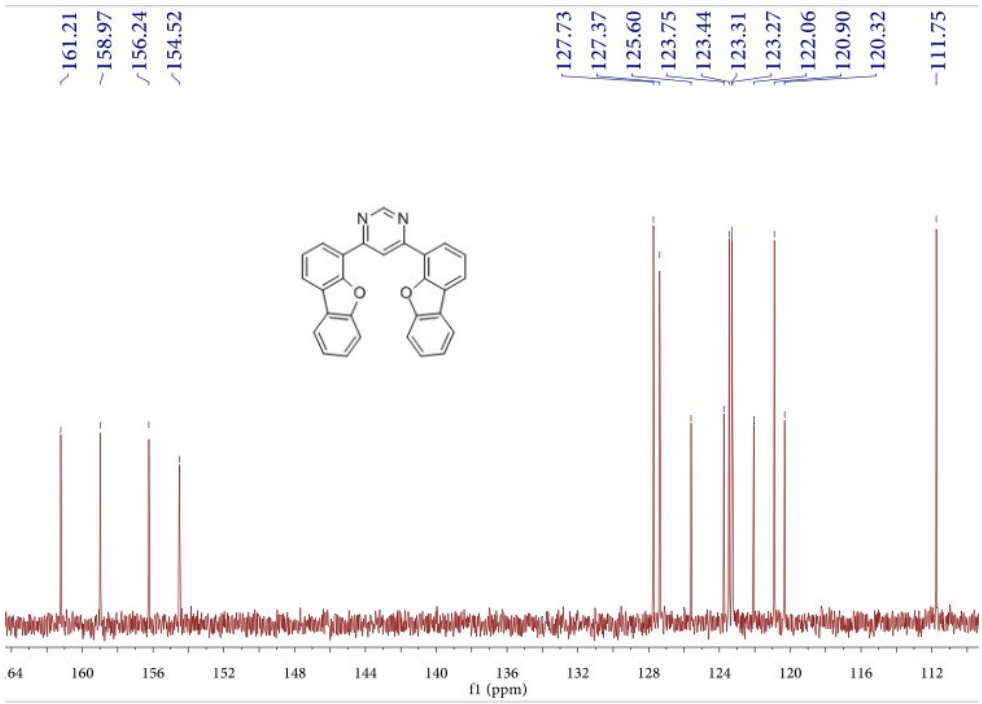


Figure S4. $^{13}C$ NMR spectrum of MDBF in $CDCl_3$.

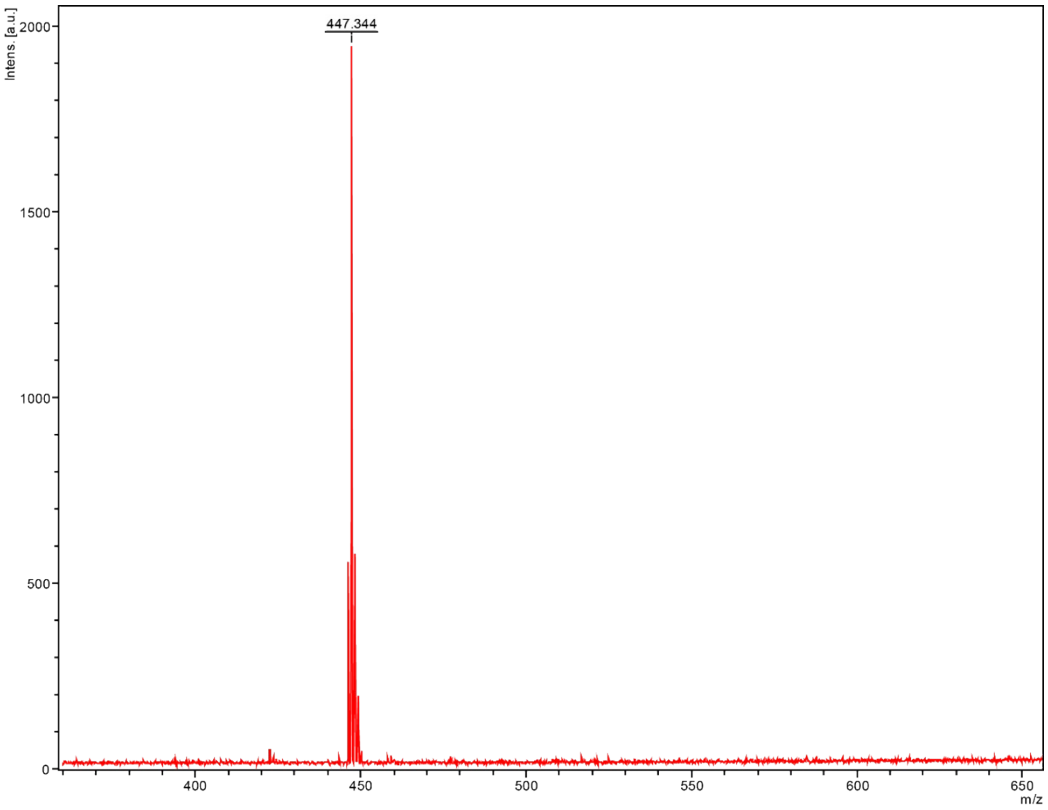


Figure S5. MALDI-TOF-MS spectrum of MDBT.

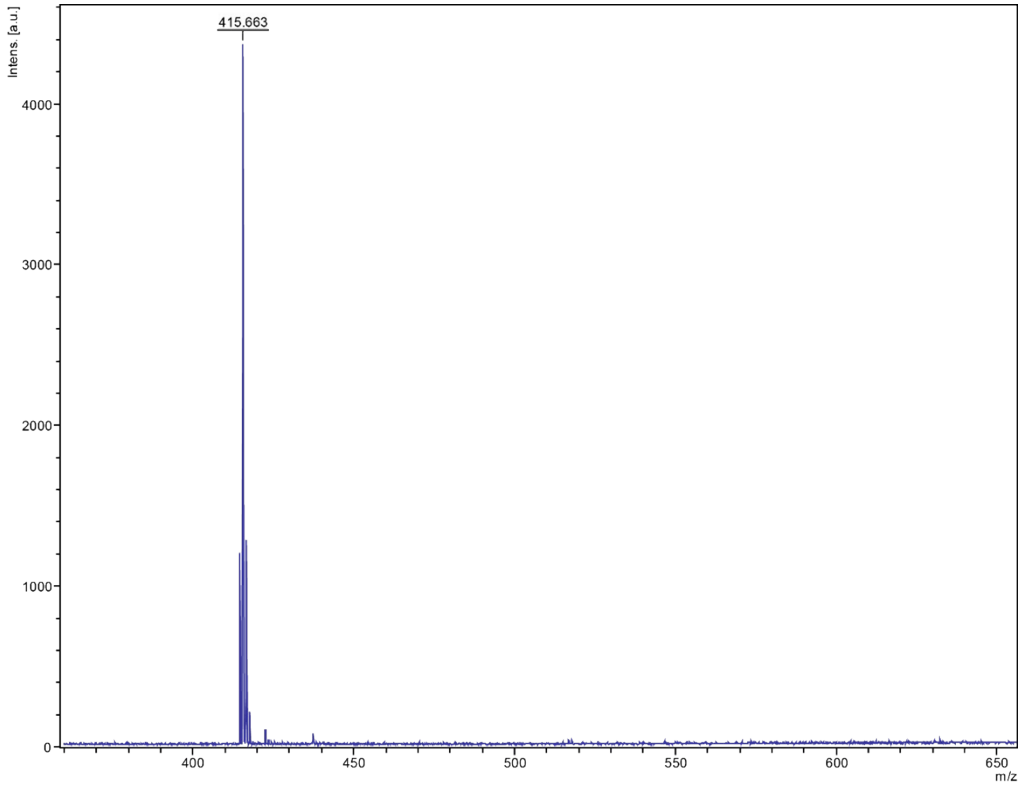


Figure S6. MALDI-TOF-MS spectrum of MDBF.

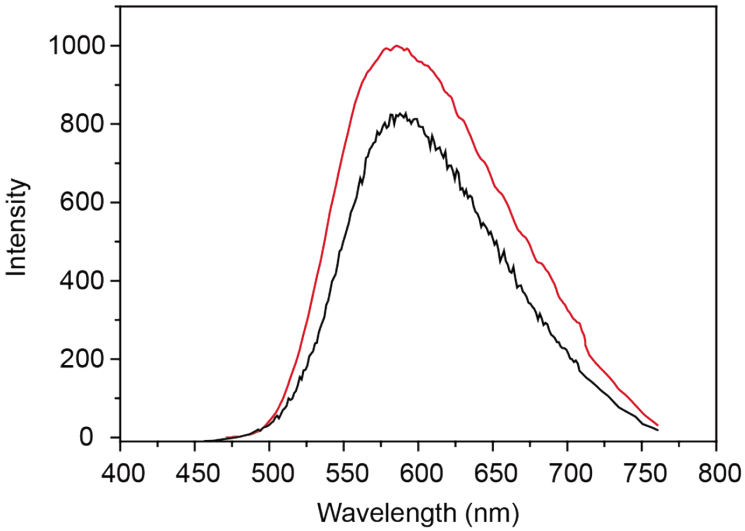


Figure S7: Phosphorescence spectra measured in air (black line) and in nitrogen (red line, rinsed with nitrogen for 30 minutes)

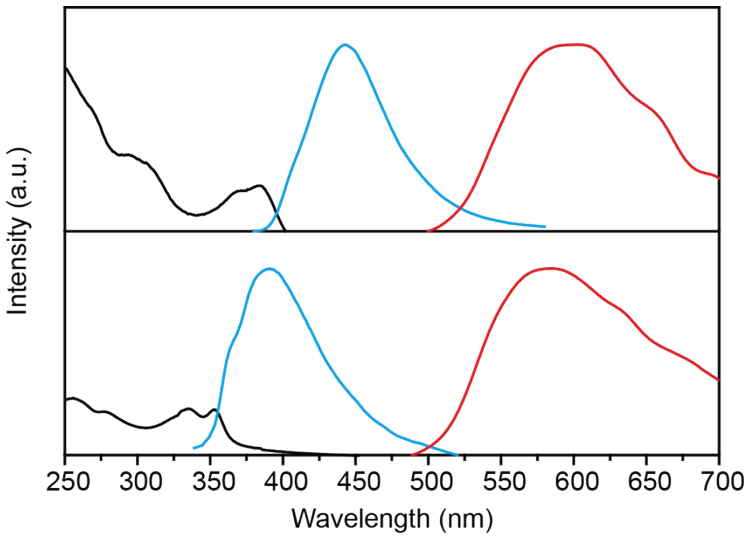


Figure S8. Ultraviolet-visible (UV-Vis) absorption, photoluminescence (PL) and phosphorescence spectra of MDBT (up) and MDBF (down) in thin film.

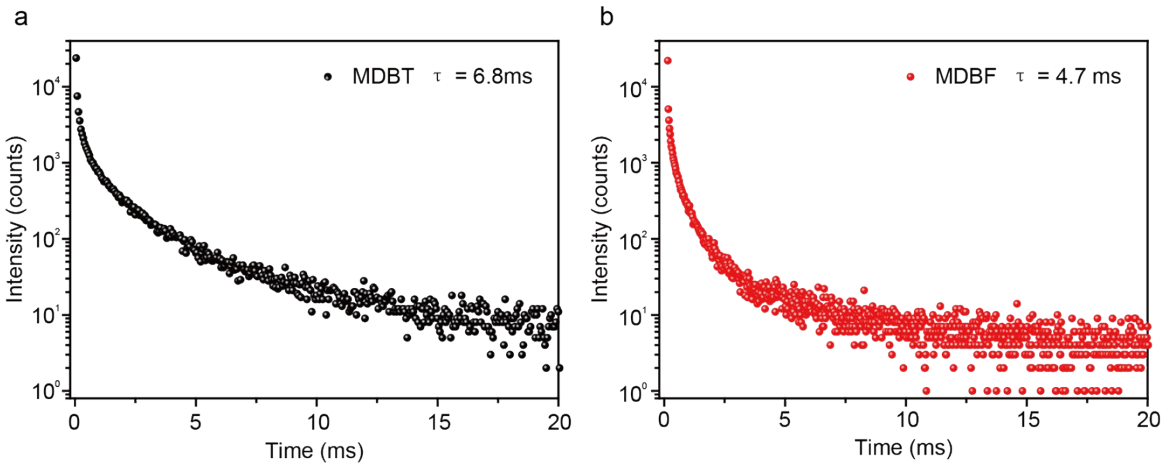


Figure S9.Phosphorescence decay profiles of MDBT and MDBF in film.

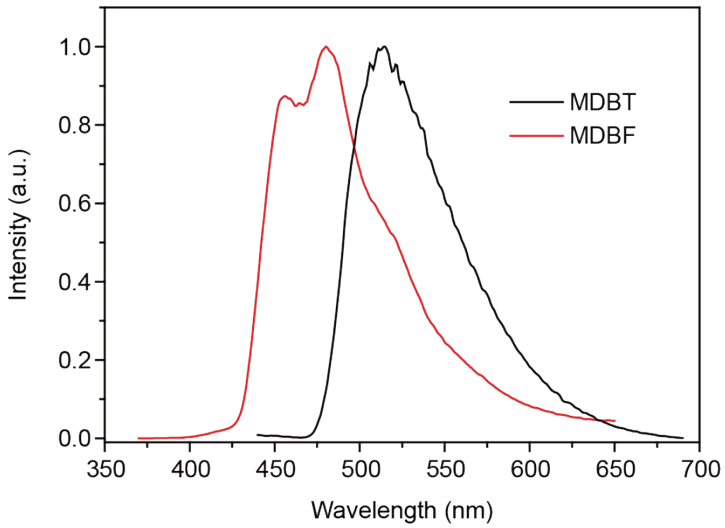


Figure S10. Phosphorescence spectra of MDBT (black line) and MDBF (red line) in solid film at 77 K.

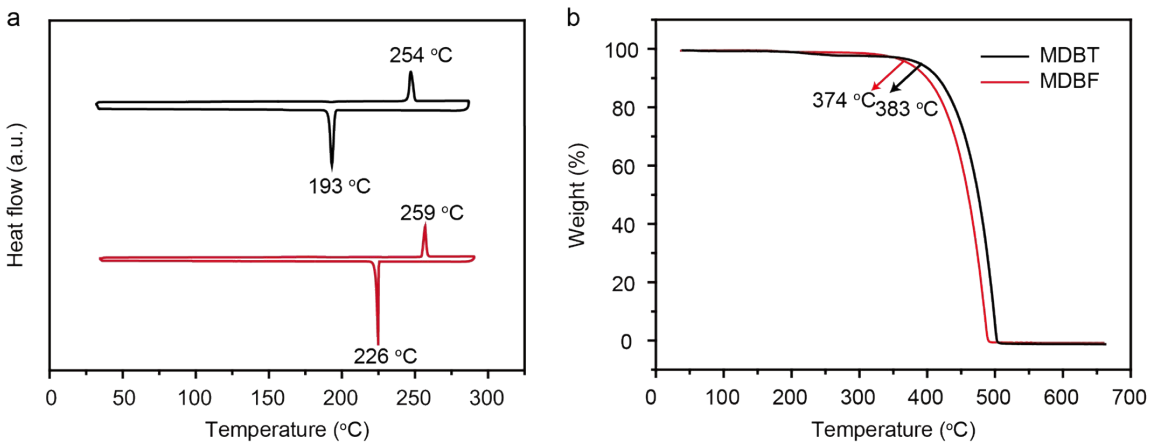


Figure S11. DSC curves (a) and TGA (b) of MDBT (black line) and MDBF (red line).

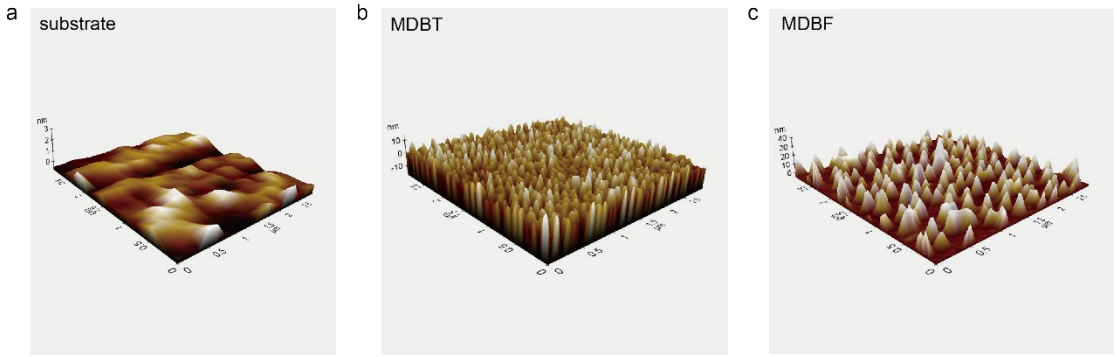


Figure S12. AFM 3D images (a: substrate, b: MDBT, c: MDBF) (the root-mean-square deviation of the substrate is 0.29 nm which will have no effect on the samples).

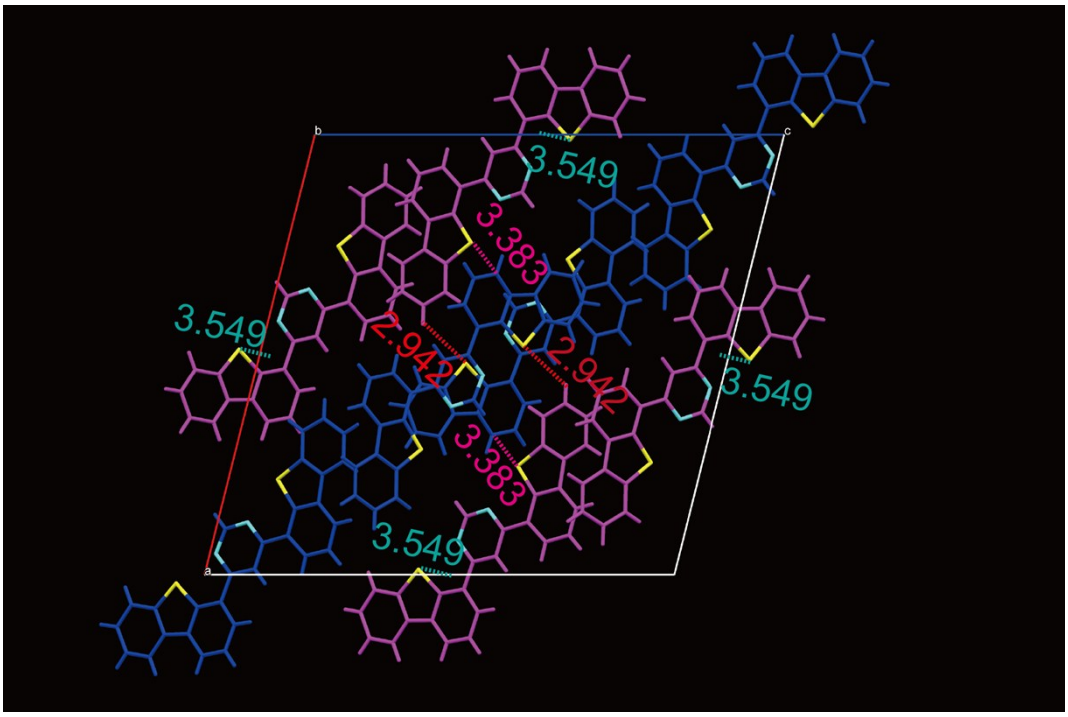


Figure S13. Molecular packing of MDBT.

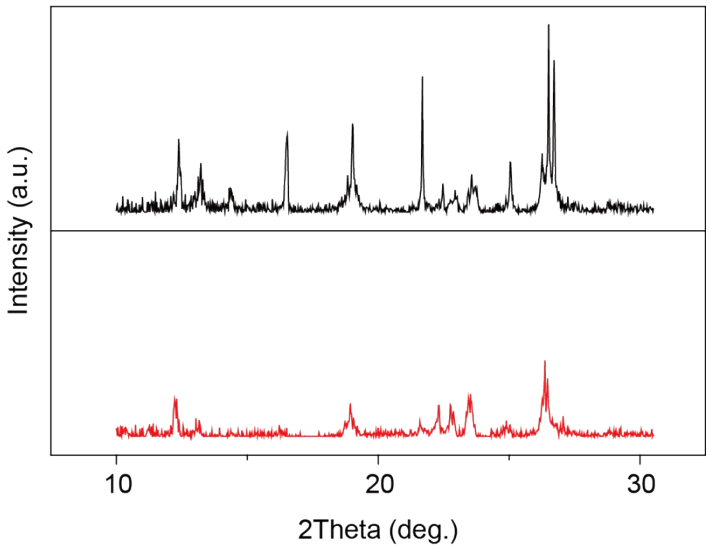


Figure S14: Powder wide-angle X-ray diffraction (PXRD) patterns of MDBT in powder (black line) and film (red line) state.

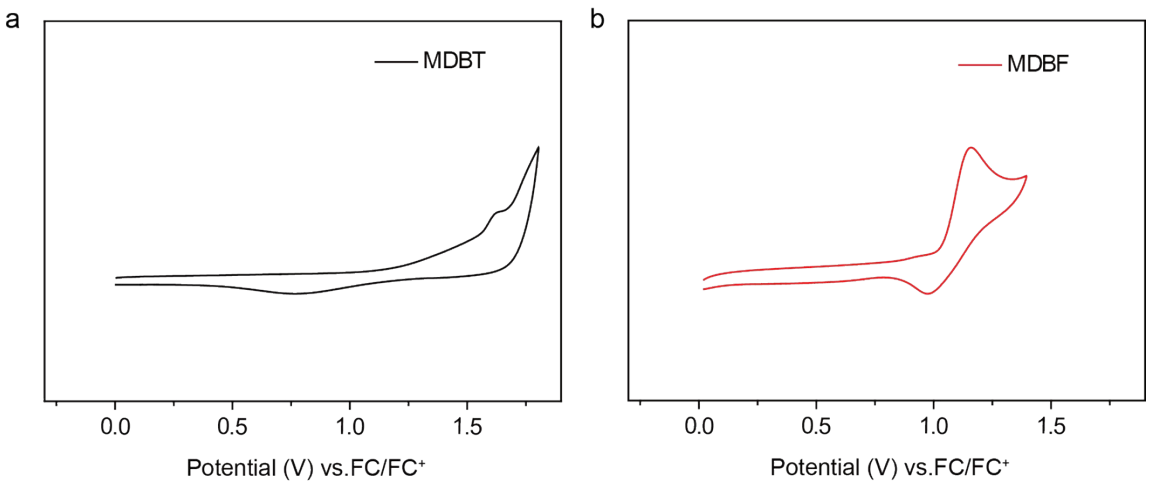


Figure S15. Cyclic voltammograms curves of a) MDBT and b) MDBF.

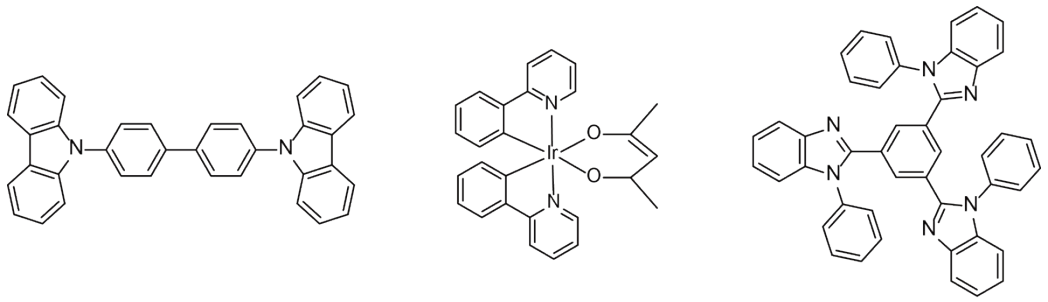


Figure S16. Chemical structures used in the device.

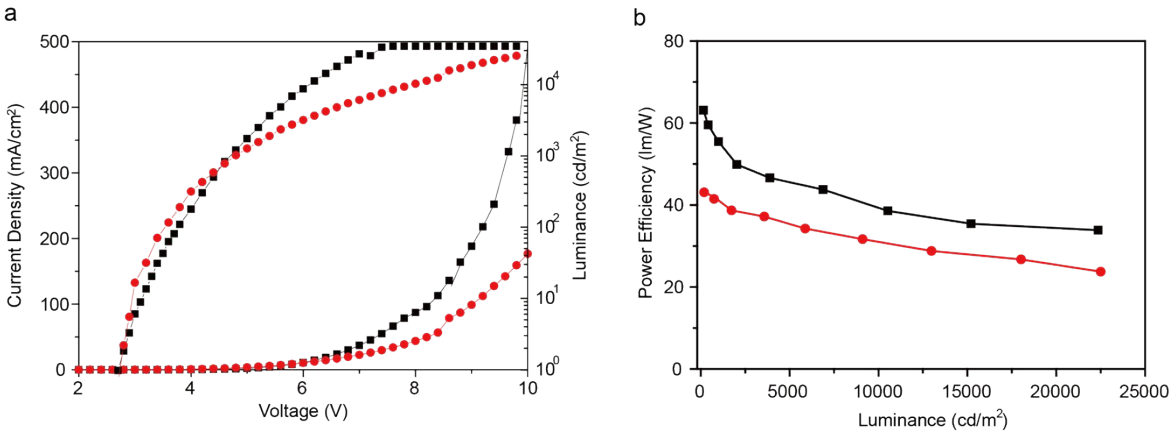


Figure S17: Current density-voltage-luminance curves (a) and power efficiency-luminance curves (b) of MDBT (black line) and MDBF (red line).

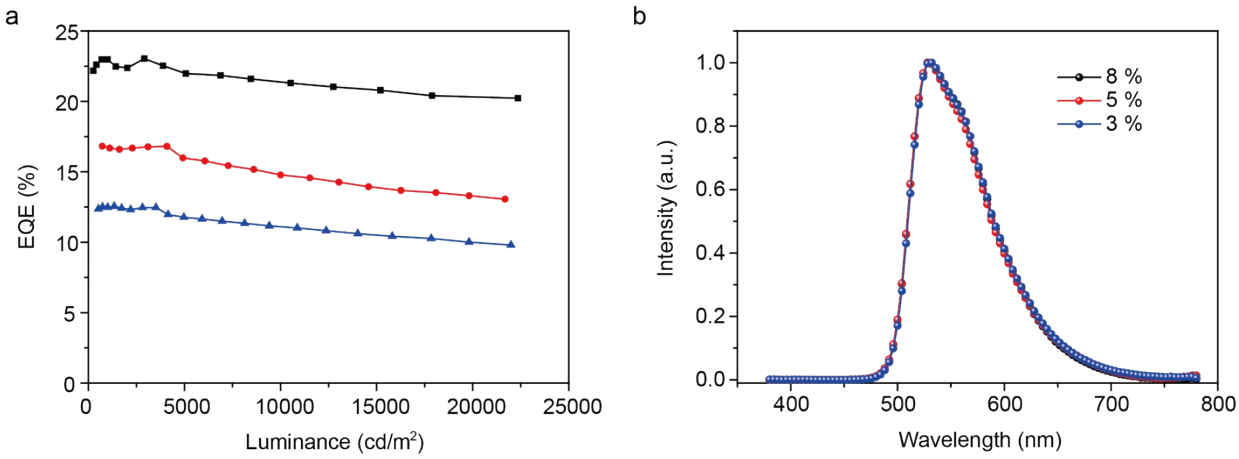


Figure S18: a) External quantum efficiency of devices with different doping ratios. b) Electroluminescence spectra of devices with different doping ratios (8 %: black line, 5 %: red line, 3 %: blue line).

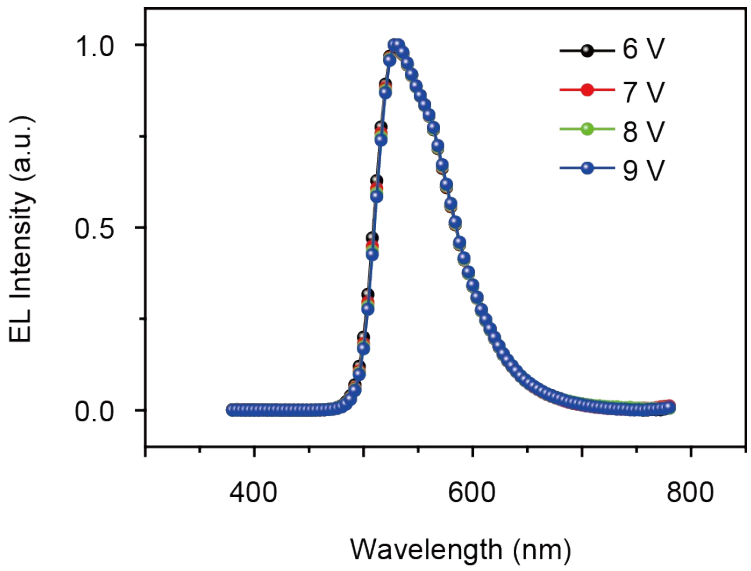


Figure S19. Electroluminescence spectra-wavelength curves of MDBT at different voltages.

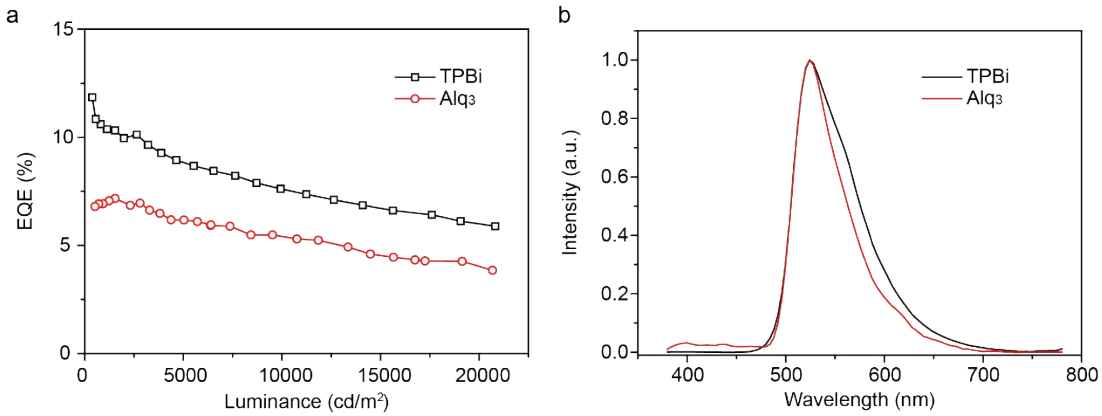


Figure S20: ITO / $MoO_3$ (1 nm) / CBP (45 nm) / MDBF: $Ir(ppy)_2(acac)$ (8%, 15 nm) / TPBi or $Alq_3$ (45 nm) / $Cs_2CO_3$ (2 nm) / Al (120 nm). a) External quantum efficiency of devices using TPBi (black line) and $Alq_3$ (red line) as electron transport layers. b) Electroluminescence spectra of devices using TPBi (black line) and $Alq_3$ (red line) as electron transport layers.

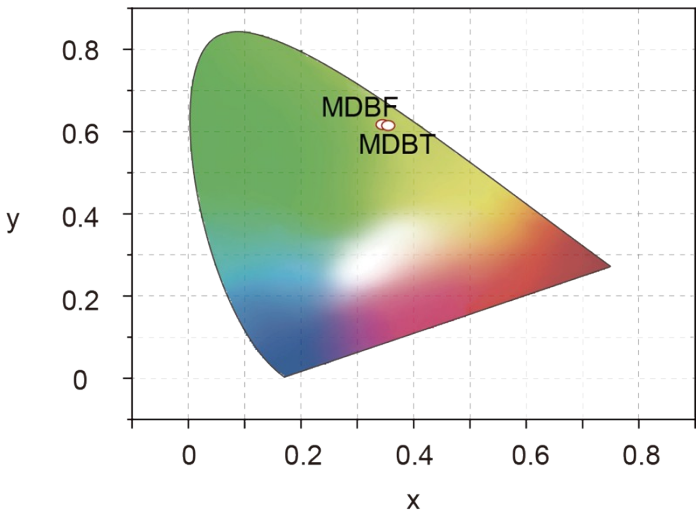


Figure S21. CIE coordinates based on MDBT and MDBF devices

1. The diffusion equation: $$n(r,t) = \frac{n_0 t_0}{t_0 + t} exp\left( - \frac{r^2}{4D(t_0 + t)} - \frac{t}{\tau} \right)$$

Here, n is the diffusion length. τ is the exciton lifetime.

2. The mobility formula: $$J_{SCLC} = \frac{9}{8}\varepsilon_0\varepsilon_r u\left(\frac{v^2}{L^3}\right)$$

Here, $J_{SCLC}$ is the current, V is the voltage, L is the thickness of the film to be tested, $\varepsilon_0$ is the vacuum dielectric constant, $\varepsilon_r$ is the relative dielectric constant, and $u$ is the carrier mobility.

Table S1. Crystallographic data for MDBT and MDBF crystals

| Compound name | MDBT | MDBF |
|---|---|---|
| Empirical formula | $C_{28}H_{16}N_2S_2$ | $C_{28}H_{18}N_2O_2$ |
| Formula weight | 444.55 | 414.44 |
| Temperature/K | 290.99 | 300.34 |
| Crystal system | monoclinic | monoclinic |
| Space group | $P2_1/n$ | $P2_1$ |
| a/Å | 22.596(11) | 3.921(4) |
| b/Å | 8.272(4) | 23.22(2) |
| c/Å | 23.381(13) | 10.935(9) |
| α/° | 90 | 90 |
| β/° | 104.048(16) | 93.07(2) |
| γ/° | 90 | 90 |
| Volume/Å$^3$ | 4240(4) | 994.4(15) |
| Z | 8 | 2 |
| $\rho_{calc}$g/cm$^3$ | 1.393 | 1.384 |
| μ/mm$^{-1}$ | 0.271 | 0.088 |
| F(000) | 1840 | 432 |
| Crystal size/mm$^3$ | 0.1 × 0.1 × 0.1 | 0.1 × 0.05 × 0.05 |
| Radiation | Mo $K_\alpha$ (λ = 0.71073) | Mo $K_\alpha$ (λ = 0.71073) |
| 2Θ range for data collection/° | 2.248 to 56.15 | 4.122 to 57.322 |
| Index ranges | -29 ≤ h ≤ 29, -10 ≤ k ≤ 10, -18 ≤ l ≤ 30 | -5 ≤ h ≤ 5, -31 ≤ k ≤ 14, -14 ≤ l ≤ 14 |
| Reflections collected | 35960 | 5200 |
| Independent reflections | 10142 [$R_{int}$ = 0.1317, $R_{sigma}$ = 0.1503] | 2729 [$R_{int}$ = 0.1037, $R_{sigma}$ = 0.1379] |
| Data/restraints/parameters | 10142/0/577 | 2729/1/289 |
| Goodness-of-fit on $F^2$ | 0.942 | 1.038 |
| Final R indexes [I>=2σ (I)] | $R_1$ = 0.0659, $wR_2$ = 0.1094 | $R_1$ = 0.0915, $wR_2$ = 0.2101 |
| Final R indexes [all data] | $R_1$ = 0.1902, $wR_2$ = 0.1431 | $R_1$ = 0.1795, $wR_2$ = 0.2523 |
| Largest diff. peak/hole / e Å$^{-3}$ | 0.30/-0.30 | 0.31/-0.32 |
| CCDC | 1942791 | 1942790 |